ChemCatChem

ChemCatChem
Chemistry Europe
European Chemical Societies Publishing

RESEARCH ARTICLE OPEN ACCESS

Heterogenized PCP Pd Pincer Complexes for the Arylation of Styrenes With Iodonium Salts

Davi S. Leite[1] | Guilherme B. Strapasson[1,2] | Leonardo S. Sousa[1] | Renato P. Murback Filho[3] | Marcos de Oliveira Junior[3] | Julio C. Pastre[1] | Daniela Zanchet[1]

[1]Institute of Chemistry, Universidade Estadual de Campinas, Campinas, SP, Brazil | [2]Brazilian Synchrotron Light Laboratory, CNPEM, Campinas, SP, Brazil | [3]São Carlos Institute of Physics, University of São Paulo, São Carlos, SP, Brazil

Correspondence: Julio C. Pastre (jpastre@unicamp.br) | Daniela Zanchet (zanchet@unicamp.br)

Received: 10 September 2025 | **Revised:** 28 November 2025 | **Accepted:** 9 December 2025

Keywords: heterogenization | Pd speciation | pincer catalyst

ABSTRACT

Phosphine-based (PCP) palladium pincer complexes, renowned for their tunable steric and electronic properties, are effective homogeneous catalysts but are prone to decomposition under the mild reductive conditions typical of cross-coupling reactions. This decomposition can generate a mixture of metal complexes and nanoparticles, complicating the rationalization of the catalytic outcome. Herein, a phosphinite Pd-POCOP-Cl complex was used to synthesize silica-supported heterogenized pincer complexes for the model arylation of *p*-bromostyrene with diphenyliodonium triflate, a reaction previously studied for its homogeneous counterpart in a proposed Pd(II)/Pd(IV) cycle but underexplored in heterogeneous catalysis. The heterogenization on SiO_2 produced surface complexes that evolved under reaction conditions, exhibiting a 15-fold higher catalytic activity than the homogeneous Pd-POCOP-Cl complex under similar conditions. This enhanced performance originated from the decomposition of the surface complexes, even in non-reductive conditions, leading to Pd leaching into the solution and forming an inactive Pd(II) species grafted onto the solid support. This transformation was facilitated by surface hydroxyl groups on SiO_2, ultimately generating soluble Pd(0) species that retained phosphorus coordination before agglomerating into nanoparticles.

1 | Introduction

Since Shaw's group's pioneering work in the 1970s, palladium pincer complexes have become indispensable in synthetic chemistry due to their robust tridentate ligand framework, which confers exceptional thermal stability, structural tunability, and reactivity [1, 2]. Also, their air- and moisture-stability makes them more practical and durable, allowing for effective transformations such as cross-coupling reactions, C-H activations, and enantioselective bond formations [3, 4]. Among these, cross-coupling reactions, vital for C-C bond formation in organic synthesis, have benefited extensively from these catalysts since Milstein et al.'s first Heck reaction report [5], leading to their use in Suzuki-Miyaura [6–8], Sonogashira [9, 10], Stille [11], Negishi [12], and Hiyama couplings [13], including carbonylative [14] and asymmetric versions [15].

A key aspect of these reactions is the role of the Pd pincer complex in the general mechanism, which remains under debate and is illustrated in Scheme 1 for phosphorus-carbon-phosphorus (PCP) pincer complexes. Studies [16–18] indicated that under the harsh conditions typical of the Heck reaction, that is, elevated temperatures (> 100°C) in highly polar solvents, the Pd complex decomposed. This normally irreversible process, driven by Pd–C bond cleavage, generates Pd(0) species, including molecular complexes, colloidal clusters, and nanoparticles (NPs). In such cases, the pincer complex served only as a precursor of the actual

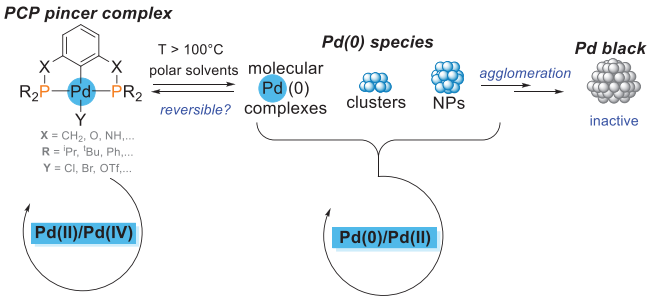

SCHEME 1 | Pincer complexes, in situ generated species, and pathways in cross-coupling reactions.

active species, Pd(0), following a Pd(0)/Pd(II) cycle. Additionally, the formation of palladium black [amorphous metallic Pd(0)], resulting from the agglomeration of Pd(0) species, was commonly observed as evidence of catalyst decomposition.

Other reports, however, suggested that pincer complexes were preserved and followed a Pd(II)/Pd(IV) cycle, although such examples remain rare in the literature [19, 20]. The introduction of carbenes in the pincer architecture, for instance, provided more stable Pd-C bonds, hindering the catalyst degradation into Pd(0) species [21, 22]. Another approach to mitigate decomposition involved conducting the reaction under an oxygen atmosphere, when compatible with the used substrates [23]. It is worth noting that the oxidation of Pd(II) to Pd(IV) in the Pd(II)/Pd(IV) cycle is thermodynamically unfavorable and typically demands strong oxidizing agents, such as hypervalent iodine reagents [24]. Nevertheless, some studies reported a Pd(II)/Pd(IV) cycle even in the absence of oxidizing agents. As an example, a recent investigation by Sabharwal et al. [25] supported the direct participation of a phosphorus-nitrogen-nitrogen (PNN) Pd complex in the Suzuki coupling of aryl halides with phenylboronic acids. Using various analytical techniques and density functional theory (DFT) calculations, the study proposed Pd(III) intermediates that were integrated into a Pd(II)/Pd(IV) cycle. The reaction, conducted in toluene at 110°C with 0.5 mol% catalyst, achieved yields of 80%–99% after 18 h.

While conventional cross-coupling reactions have been extensively studied, the use of strong oxidants to promote a predominant Pd(II)/Pd(IV) cycle remains relatively unexplored in the literature. A notable example is the work of Aydin et al. [26] using homogeneous catalysis, employing Pd PCP and nitrogen-carbon-nitrogen (NCN) pincer complexes in the Heck-type arylation of alkenes using iodonium salts as arylating agents. Their approach demonstrated high chemoselectivity and compatibility with sensitive functionalities such as allylic acetates and aryl bromides. Catalyst integrity was confirmed via ^{31}P NMR and mercury-drop tests, ruling out the presence of active Pd(0) species. The reaction achieved yields of 74%–99% using 5 mol% Pd in THF or acetonitrile at 50°C over 16 h. While these conditions required a higher catalyst loading than conventional Heck reactions, they enabled significantly milder reaction temperatures [16].

Further insights into the Pd(II)/Pd(IV) pathway were provided by Szabó [27], who investigated the oxidative addition of hypervalent iodonium salts to Pd(II) pincer complexes. This step was identified as exothermic and irreversible, with a low activation barrier dependent on the organic substituents. Such irreversibility facilitates key catalytic processes, including ligand exchange and transmetallation, which enables the formation of stable Pd(IV) intermediates and broadens the scope of Pd-catalyzed transformations. Complementary findings by Canty and Ariafard [28] highlighted the mechanistic complexity of Pd(II)/Pd(IV) cycles, showing that $NaHCO_3$, a commonly used base, can induce a competing reduction pathway back to Pd(0) by attacking the pincer ligand. This raises the possibility of Pd NPs formation under these conditions, further complicating the mechanistic landscape.

Beyond their role in homogeneous catalysis, significant research has focused on the heterogenization of pincer complexes through immobilization strategies to enhance catalyst separation and enable continuous processing. These strategies have addressed both non-covalent and covalent attachment to organic supports (*e.g.*, polymers, resins, dendrimers) [29–31] and inorganic supports (*e.g.*, oxides, clays, carbon nanotubes) [32–34], with covalent anchoring onto inorganic supports showing the greatest promise for efficient catalyst recovery [35]. However, immobilization further complicates cross-coupling reactions, as the mechanistic role of the immobilized Pd catalyst remains debated, involving both solid-phase and leached species. Some studies suggested that immobilized complexes acted primarily as Pd(0) reservoirs, releasing active species into solution [36–38], while others provided evidence for genuinely heterogeneous catalytic mechanisms [39, 40]. Moreover, as in homogeneous systems, heterogenized catalysts, including those beyond the pincer family, often generate a complex mixture of soluble molecular complexes, clusters, and nanoparticles due to leaching, complicating the identification of the true active species and hindering the rationalization of catalytic behavior [41].

In the specific case of heterogeneous cross-couplings using hypervalent iodonium salts as oxidizing arylating agents, Vadulla et al. [42] explored a dopamine-functionalized Fe_3O_4-supported Pd catalyst, achieving 65%–90% yield in the arylation of terminal alkenes within 5 min under base-free conditions, with no detectable leaching. Similarly, Perez et al. [43] developed a Heck-arylation/cyclization method for 4-arylcoumarin synthesis using PdO/Fe_3O_4 catalyst, obtaining 40%–98% yield under mild conditions. However, in this case, catalyst recyclability was limited due to Pd reduction and iodine poisoning, with 4% Pd leaching detected.

Here, we introduce a heterogeneous approach for the model arylation of *p*-bromostyrene with diphenyliodonium triflate under mild conditions, a reaction traditionally associated with a Pd(II)/Pd(IV) cycle in homogeneous systems. We used a phosphinite-based PCP Pd pincer complex, $(Ph_2PO)_2$-C_6H_4-Pd-Cl (referred to as Pd-POCOP-Cl), as a precursor for silica-immobilized catalysts (denoted PCP-Pd/SiO_2), containing 1 wt.% Pd. We demonstrate that the interaction between the pincer complex and the silica support in the reaction medium generates highly active catalytic species that exhibit remarkable activity even at low catalyst loadings. This work provides an investigation into the nature, formation pathways, and catalytic behavior of these active species.

TABLE 1 | Optimization of the reaction conditions.

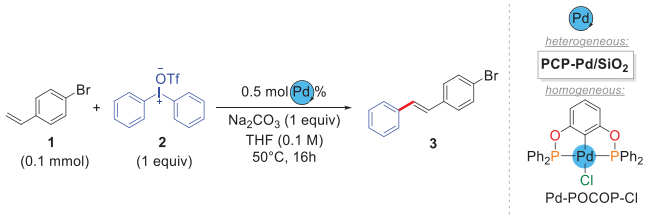

Entry	Variation from "standard" conditions[a]	Yield 3[b]
1	None	62
2	Pd-POCOP-Cl instead of PCP-Pd/SiO_2	4
3	SBA-15 instead of fumed SiO_2	59
4	1.5 equiv of **2**	65
5	$NaHCO_3$ instead of Na_2CO_3	63
6	NMP instead of THF	67
7	DMF instead of THF	31
8	2 equiv of base	61
9	room temperature instead of 50°C	15
10	1 mol% Pd instead of 0.5 mol% Pd[c]	35
11	argon atmosphere	58
12	PhI instead of Ph_2IOTf	*traces*
13	physical mixture of Pd-POCOP-Cl and SiO_2 instead of PCP-Pd/SiO_2	3

[a]Standard conditions: 0.5 mol% Pd, using a PCP-Pd/SiO_2 catalyst supported in fumed AEROSIL SiO_2 with 1 equivalent of Na_2CO_3 in THF (0.1 M) at 50°C for 16 h.

[b]Yield determined by GC-MS using naphthalene as internal standard. Only minor traces of diarylated product were detected. The data corresponds to the average of duplicate experiments, showing agreement within a 10% error margin.

[c]Performed with twice the catalyst amount, while maintaining 1 wt.% Pd.

2 | Results and Discussion

2.1 | Catalytic Evaluation

The arylation of styrenes using iodonium salts has been extensively investigated in literature in terms of substrate scope, including variations in steric and electronic properties [24]. To enable a focused and detailed comparison of the catalytic performance of homogeneous and heterogeneous systems, we selected the model reaction between *p*-bromostyrene and diphenyliodonium triflate. The heterogenization of Pd-POCOP-Cl was obtained by producing a Pd/silica catalyst with 1 wt.% Pd loading by wet impregnation in commercial silica (PCP-Pd/SiO_2). The details of catalyst preparation are presented in the Supporting Information.

Representative examples of reaction condition optimization are summarized in Table 1, with additional conditions provided in the Supporting Information (Table S1 and Figures S1 and S2). The optimal conditions using PCP-Pd/SiO_2 were determined to be a reaction in THF at 50°C, employing 1 equivalent of diphenyliodonium triflate and 1 equivalent of Na_2CO_3 as the base (entry 1). Under these conditions, the analysis by gas chromatography-mass spectrometry (GC-MS) revealed a 62% yield of *p*-bromostylbene as the primary product after 16 h, as shown in the Supporting Information section (Figures S3–S5). Under similar conditions, the homogeneous reaction (entry 2) yielded only 4% of the product. Comparable results were obtained using mesoporous SBA-15 as support (entry 3), indicating similar catalytic species.

Increasing the amount of the arylating agent (Table 1, entry 4) or replacing Na_2CO_3 with $NaHCO_3$ (Table 1, entry 5) did not lead to a significant improvement in product yield. Attempts to enhance the reaction yield using other solvents commonly applied in cross-coupling reactions resulted in only a slight improvement for NMP (Table 1, entry 6) or reduced the yield by half for DMF (Table 1, entry 7). Increasing the base equivalents also had no noticeable effect on yield (Table 1, entry 8), consistent with the limited solubility of the base in THF. Lowering the reaction temperature to room temperature decreased the yield to 15% (Table 1, entry 9). Doubling the catalyst loading (Table 1, entry 10), by employing more catalyst yet maintaining 1 wt.% Pd, unexpectedly reduced the catalytic efficiency, which could be attributed to possible mass transfer limitations or to potential Pd aggregation, already observed in other heterogeneously catalyzed cross-coupling reactions [44]. Additionally, conducting the reaction under inert argon atmosphere (Table 1, entry 11) similarly showed no improvement in yield, suggesting that oxygen did not play a significant role in the catalytic process. Replacing the iodonium salt with iodobenzene (Table 1, entry 12) resulted in only trace amounts of the product, indicating that the reaction mechanism differs from the conventional Mizoroki-Heck pathway.

Substituting the heterogeneous PCP-Pd/SiO_2 catalyst with a physical mixture of the complex with the silica support (Table 1, entry 13) yielded 3% of the desired product. This indicates a distinct reaction pathway when the heterogeneous catalyst was employed. Furthermore, as detailed in the Supporting Information, even $Pd(OAc)_2$ (Table S1), a commonly used Pd source for such reactions, failed to efficiently catalyze the reaction under these conditions. As shown, the heterogeneous PCP-Pd/SiO_2 catalyst exhibited approximately 15 times higher yield than its homogeneous counterpart, prompting a deeper investigation into the catalyst's structural nature and its evolution throughout the reaction process.

2.2 | Catalyst Characterization

The heterogeneous catalyst was characterized to determine the nature of the species formed following the impregnation process of the Pd-POCOP-Cl complex on SiO_2, described in the Supporting Information. Scheme 2 illustrates the possible outcomes of the wet impregnation process. One of them involves the formation of a non-covalently immobilized Pd-POCOP-Cl complex (O1 in Scheme 2), where the complex remained structurally intact and stabilized through intermolecular interactions such as hydrogen bonding and dispersion forces. Another scenario involves grafting the complex onto the silica surface via substitution of the chloride ligand with a siloxyl group derived from the abundant surface hydroxyl groups of the support, resulting in a surface-anchored complex (O2 in Scheme 2). Additionally, the inherent tendency

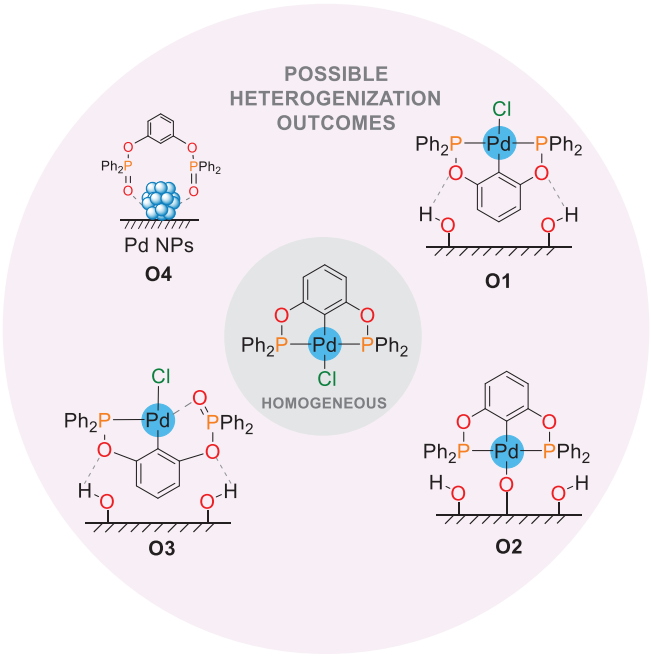

SCHEME 2 | Homogeneous Pd-POCOP-Cl and possible heterogenization outcomes (O1-O4) after wet impregnation on SiO_2.

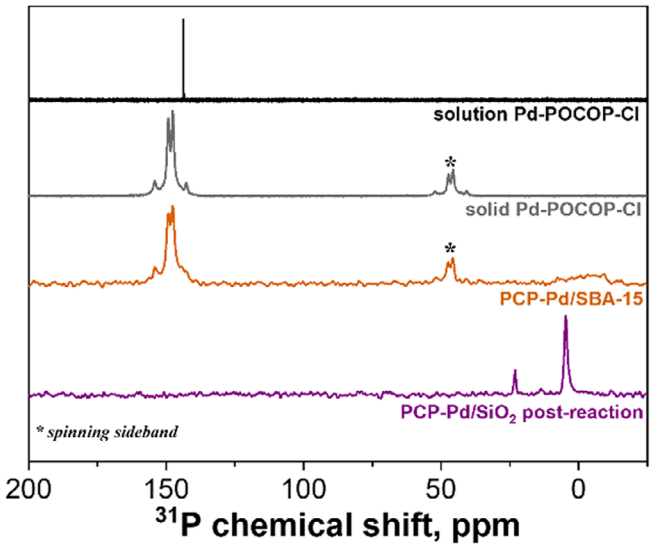

FIGURE 1 | ^{31}P NMR spectra for Pd-POCOP-Cl (proton-decoupled, $CDCl_3$, 25°C, 101.3 MHz), solid-state (CP-MAS, 243.2 MHz, 10 Hz spinning) for Pd-POCOP-Cl, PCP-Pd/SBA-15 heterogeneous catalyst, and PCP-Pd/SiO_2 post reaction.

of Pd to undergo reduction, coupled with the oxidation of the phosphine arm, could lead to partially decomposed species, such as O3, which retained the structure of a metal complex. Further decomposition could progress to the formation of Pd NPs, accompanied by the oxidized phosphine form of the PCP ligand (O4 in Scheme 2).

Figure 1 presents the ^{31}P NMR spectra of the Pd-POCOP-Cl complex in $CDCl_3$ solution, its solid-state form, a freshly prepared heterogeneous catalyst, and a post-reaction catalyst. In solution, Pd-POCOP-Cl displayed a single sharp resonance at 143 ppm, consistent with a well-defined pincer coordination environment. In the solid state, two distinct signals appeared at 147.0 and 149.4 ppm, also exhibiting hyperfine coupling to ^{105}Pd, indicative of preserved Pd-P coordination. The presence of two signals may reflect distinct conformers or packing-induced distortions in the solid lattice. After impregnation, these spectral features were retained, indicating that the pincer coordination remained intact in the supported material (see also Figure S8). A weak additional resonance near 0 ppm emerged, which is likely attributed to minor phosphine degradation, potentially arising from the hydrolytic cleavage of the P-C bond. Similar patterns have been observed in related immobilized Ir-POCOP-CO and Ir–POCOP–ethylene systems [45], where the presence of spinning sidebands for only some of the signals was associated with the restricted mobility of the pincer complexes on the silica surface. Importantly, the absence of a resonance around 30 ppm, characteristic of the phosphine oxide derivative of the POCOP ligand, suggests that oxidative degradation was minimal and that the pincer scaffold remained largely intact after impregnation. The ^{31}P NMR spectrum of the post-reaction PCP-Pd/SiO_2, however, showed that the original high-field resonances disappeared, replaced by two new signals at 23 and 4.5 ppm. These shifts were consistent with the formation of adsorbed diphenylphosphine oxide ($Ph_2P(O)H$) and Pd(II)-phosphinate species, respectively, as previously reported for decomposed Ir-POCOP-Cl immobilized in silica and alumina [46]. This transformation indicated that the original Pd–POCOP structure underwent extensive structural changes during the catalytic process.

X-ray photoelectron spectroscopy (XPS) spectra of the Pd 3d region of the Pd-POCOP-Cl complex (Figure 2) present peaks at 338.3 and 343.6 eV, corresponding to Pd $3d_{5/2}$ and Pd $3d_{3/2}$ contributions, respectively. The narrow peaks (FWHM Pd $3d_{5/2}$ = 1.3 eV) indicate that the Pd chemical environment was homogeneous and consistent with a Pd(II) oxidation state, with a binding energy associated with a Pd-Cl bond [47, 48]. The XPS signals for chlorine, phosphorus, carbon, and oxygen of the Pd-POCOP-Cl complex are presented in Figure S6 and were consistent with the molecular structure. Table S2 presents the surface atomic concentration, confirming the expected molar ratio of Pd:P:Cl as 1:2:1. In the case of the PCP-Pd/SiO_2, XPS revealed two Pd entities (Figure 2). The main peak, characterized by a maximum at 338.5 eV, corresponds to the non-covalent immobilization of the pincer complex (Scheme 1, O1). The presence of another peak at 336.7 eV, however, demonstrated that a fraction of ca. 30% of the Pd had a different coordination environment. The new peak position was consistent with Pd(II) coordinated to oxygen [46, 48, 49], indicating that a fraction of the complex was grafted onto the surface, as in the structure of O2 in Scheme 1. Previous work demonstrated similar behavior for Ir-POCOP complexes, in which both grafted and hydrogen-bonded complexes could be detected during catalyst immobilization in silica [46]. The broadening of the peaks also suggests that Pd was interacting with the support, corroborating its immobilization on the surface of SiO_2. The XPS signals for chlorine and phosphorus in the PCP-Pd/SiO_2 catalyst were below the detection limit due to the high background signal generated by the SiO_2 support and could not be analyzed. Additional XPS discussion of the other core elements is provided in the Supporting Information (Section 4, Table S2, Figures S6 and S7). As already pointed out by the ^{31}P NMR, the XPS spectra of the post-reaction PCP-Pd/SiO_2

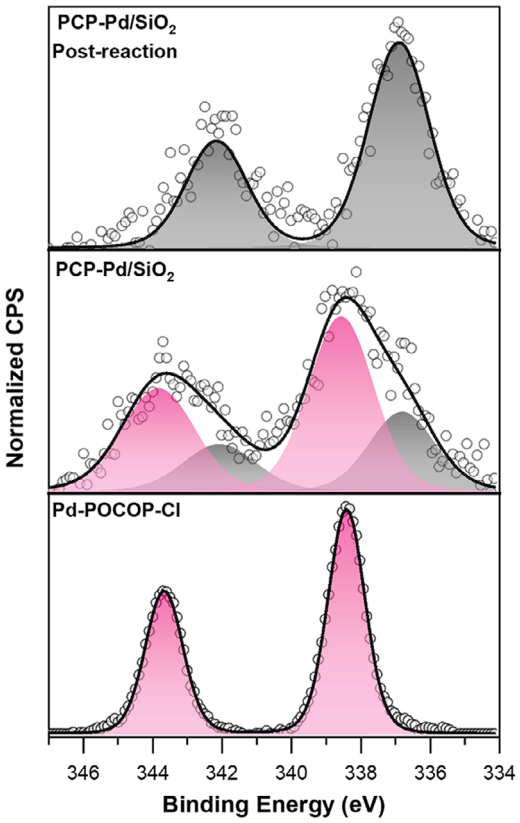

FIGURE 2 | Pd 3d XPS spectra of Pd-POCOP-Cl, PCP-Pd/SiO_2 (fresh), and PCP-Pd/SiO_2 post-reaction. The pink curve corresponds to Pd(II)-Cl species, while the gray represents Pd species coordinated to oxygen atoms.

confirmed the complete transformation of the Pd species to the Pd(II) coordinated to an oxygen environment induced by the reaction conditions.

CO adsorption/diffuse reflectance infrared spectroscopy (CO-DRIFTS) was employed in the fresh PCP-Pd/SiO_2 catalyst to verify the presence of metallic Pd species. The C–O stretching frequency observed upon CO binding to Pd is highly sensitive to the binding configuration and the specific Pd site involved, providing a valuable probe for structural characterization. As shown in Figure 3a, the surface complex remained stable during the dehydration step to 150°C, a necessary preparation for CO-DRIFTS measurements. Only bands corresponding to free CO, originating from excess gas within the chamber, were detected, with no evidence of chemisorbed CO (Figure 3b,c), indicating the coordinative saturation of the species formed during the impregnation step. These results further support the XPS and NMR findings, confirming that the impregnation process preserved the structural integrity of Pd-POCOP framework, while forming both hydrogen-bonded complexes and physiosorbed species on the surface, with no evidence of Pd NP formation.

2.3 | Mechanistic Studies

To gain deeper insight into how the immobilized complexes contribute to the observed catalytic activity and the stability of the catalyst in the reaction medium as a function of time, we monitored the reaction progress and correlated it with spectroscopic data. UV-Vis absorption and liquid-phase ^{31}P NMR spectra were used to analyze aliquots at different time intervals after removal of insoluble components. As shown in Figure 4a, the product yield gradually increased, starting at approximately 38% yield after 1 h, reaching 59% after 6 h, and stabilizing at 62% after 12 h.

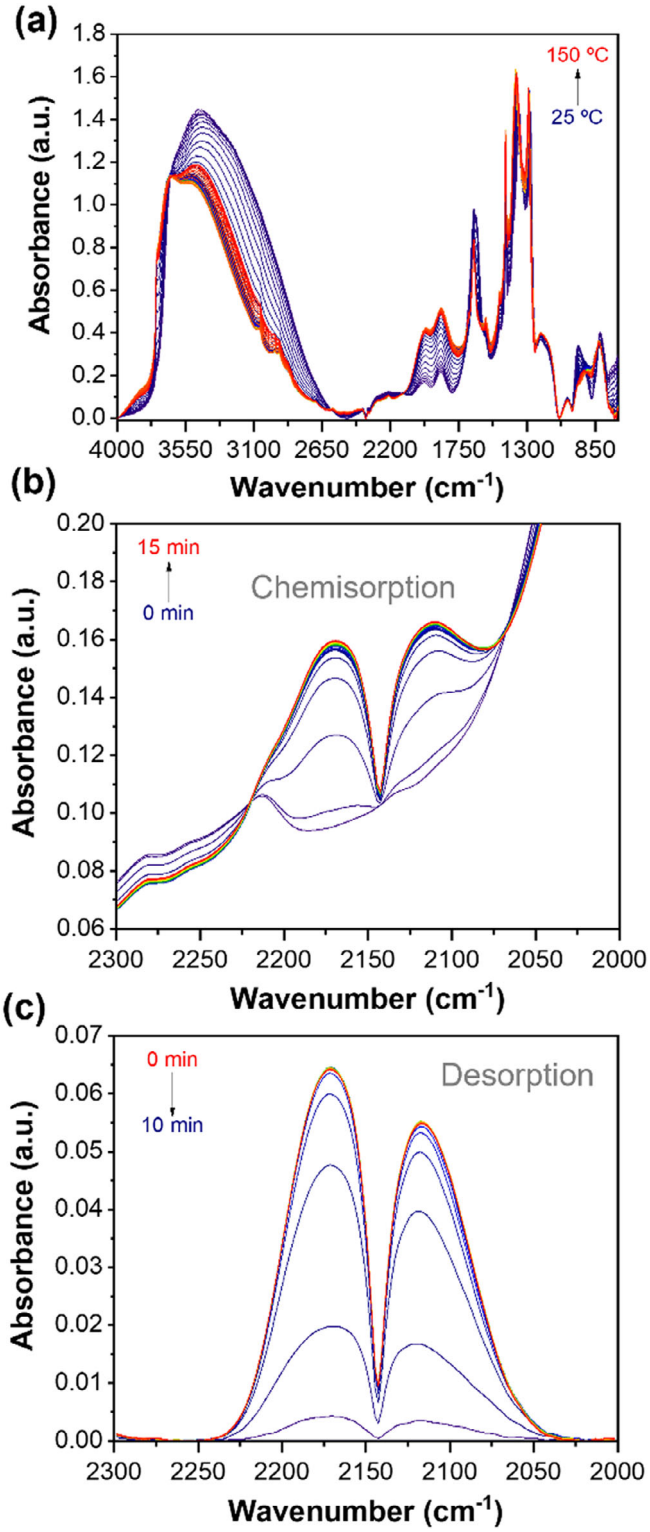

FIGURE 3 | CO DRIFTS spectra for the fresh PCP-Pd/SiO_2 catalyst showing (a) in situ dehydration under heating, (b) CO chemisorption at room temperature, and (c) CO desorption.

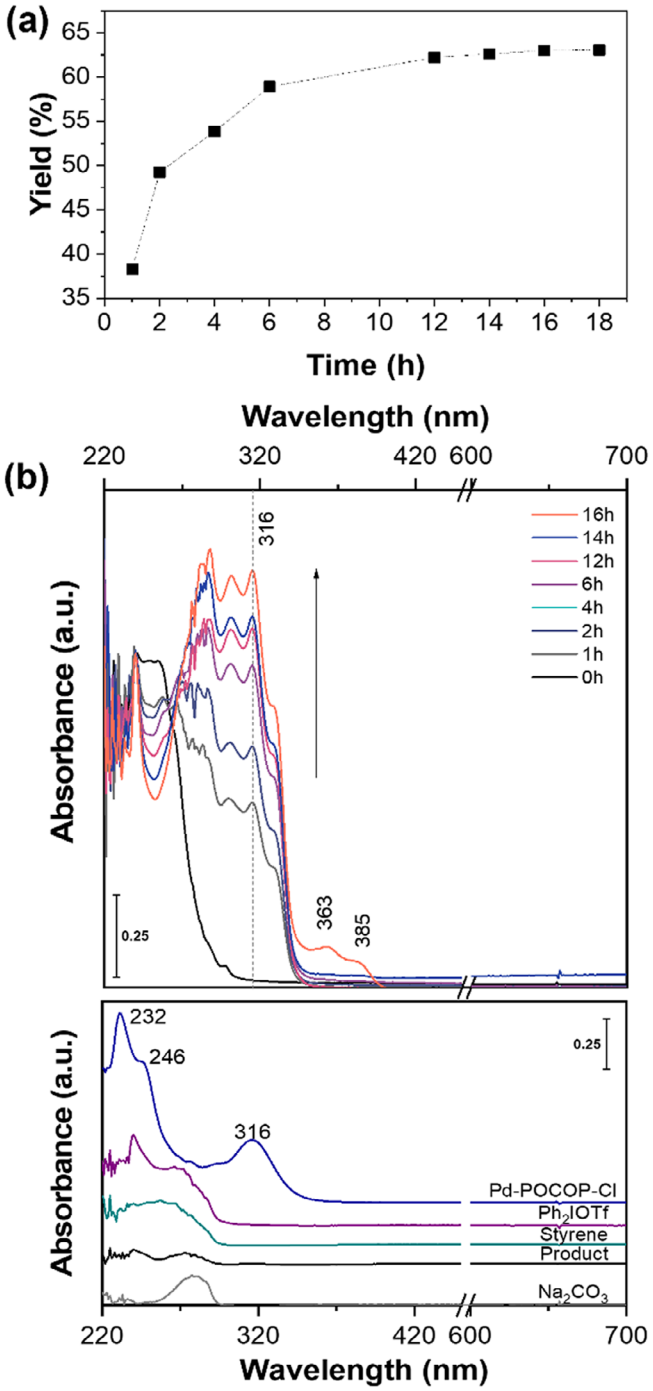

FIGURE 4 | (a) Reaction product yield over time. (b) UV-Vis absorption spectra of liquid aliquots collected during the arylation of p-bromostyrene with diphenyl iodonium triflate using PCP-Pd/SiO_2 as the catalyst (top) and separate reaction components (bottom).

Figure 4b presents the UV-Vis spectra of liquid aliquots during the reaction, showing the evolution of the reaction medium over time (top), and the spectra of separate reaction components and homogeneous Pd-POCOP-Cl complex (bottom). The spectrum of Pd-POCOP-Cl was characterized by two interligand π–π^* bands at 232 and 246 nm, along with a ligand-to-metal charge transfer (LMCT) band at 316 nm [50]. The spectra of the starting materials and the product also exhibited strong π–π^* transitions below 300 nm. For the reaction aliquots, a complex mixture of bands

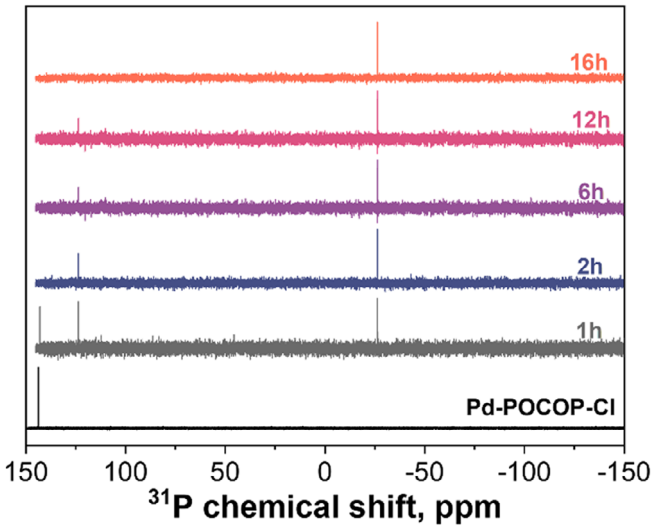

FIGURE 5 | ^{31}P NMR spectra at 500 MHz of the liquid samples in $CDCl_3$, 25°C, during the arylation of p-bromostyrene and diphenyliodonium triflate using PCP-Pd/SiO_2 as catalyst.

in the 300–350 nm range was observed, likely associated with leached Pd(II) species. Among these, the 316 nm band remained visible, suggesting that some species retain the pincer ligand as Pd-POCOP-Cl.

The formation of colloidal Pd clusters is typically evidenced in UV-Vis spectra by the appearance of a shoulder in the 370–390 nm region, corresponding to plasmon resonance excitation [51–53]. In our case, no distinct plasmon shoulder was initially observed in this region. However, after 16 h of reaction, a pronounced shoulder developed in this region, as highlighted in Figure 4b (bottom), suggesting the gradual formation of Pd clusters over time. Also, a marked darkening of the reaction medium was observed, consistent with the formation of insoluble Pd black. These observations suggest that colloidal Pd clusters form progressively during the reaction and eventually agglomerate into larger, insoluble Pd black particles.

The same aliquots were submitted to ^{31}P NMR analysis, shown in Figure 5. After 1 h of reaction, the spectrum exhibited a signal corresponding to leached Pd-POCOP-Cl (143 ppm) complex and two additional resonances at 124 and -26 ppm. The signal at -26 ppm matched the presence of polyphosphates, likely originating from the condensation of leached ligand decomposition products [54, 55]. This signal persisted throughout the reaction. Despite extensive efforts to isolate the species formed at the beginning of the reaction, we were unable to satisfactorily assign a definitive structure to the 124 ppm signal. Melero et al. [56] demonstrated that PCP pincer Pd hydroxo complexes, in the presence of alcohols such as methanol or isopropanol, form well-defined dimeric or polymeric Pd(0) bridging complexes. Their study suggested that these species arise from the decomposition of a Pd(IV) hydride intermediate, driven by the interaction with the hydroxyl groups of the alcohol. This transformation was characterized by a ^{31}P NMR chemical shift, showing an 18-ppm downfield shift from 57 ppm in the Pd(II) hydroxo complex to 39 ppm in the dimeric Pd(0) complex. In Figure 5, the observed signal at 124 ppm

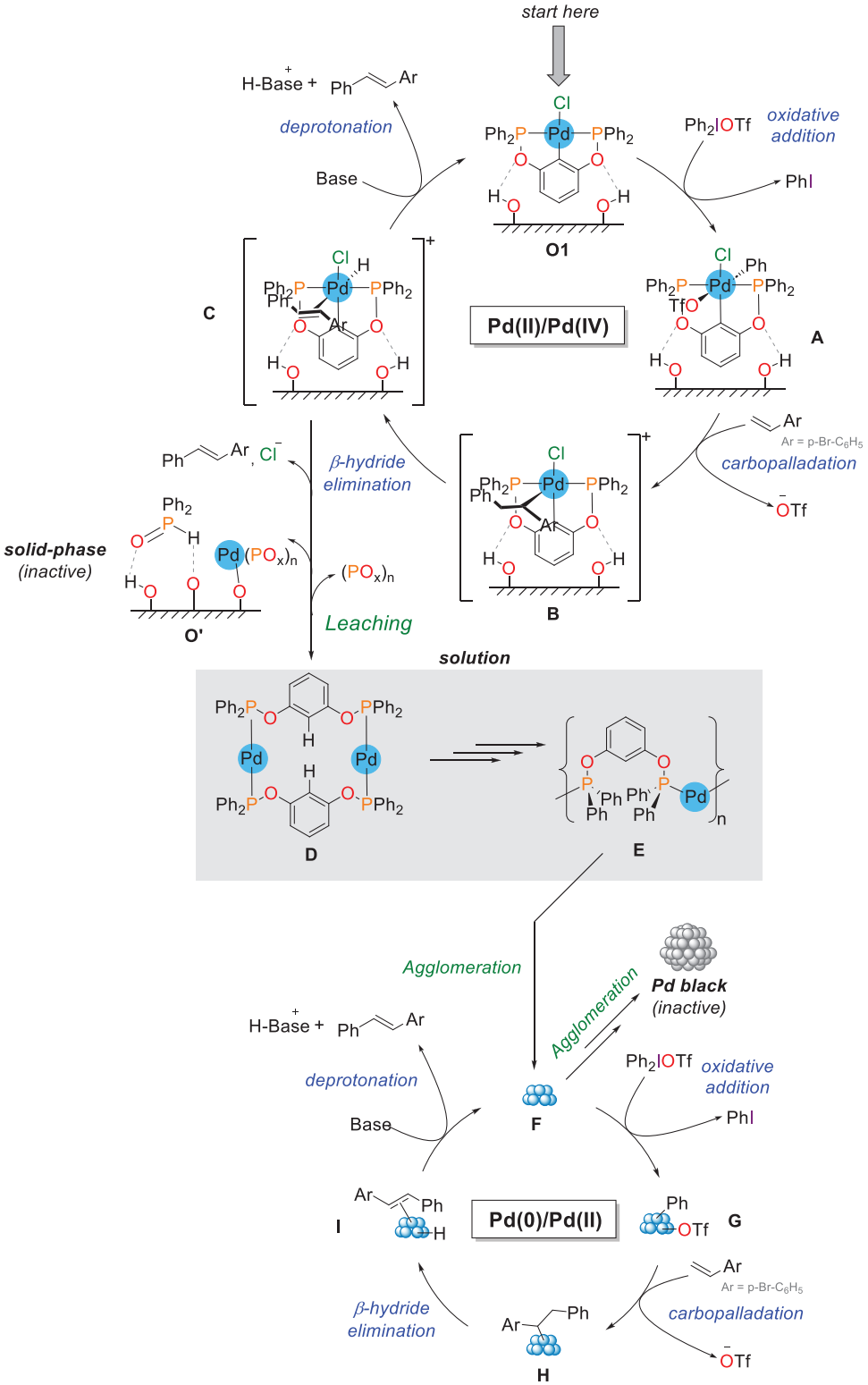

SCHEME 3 | Proposed catalytic cycle for the arylation of p-bromostyrene and diphenyliodonium triflate using PCP-Pd/SiO_2 as catalyst.

was 19 ppm downfield from the homogeneous Pd-POCOP-Cl complex (143 ppm) and may correspond to the –OPh_2P–Pd(0)–PPh_2O– fragment. This indicated the formation of dimeric or polymeric Pd(0) bridging complexes, as highlighted in gray in Scheme 3, which is consistent with the NMR of other complexes with similar structures [57, 58]. In contrast to the homogeneous case [56], the surface hydroxyl groups of the support in our system likely played a role analogous to that of alcohols.

Complementary inductively coupled plasma optical emission spectroscopy (ICP-OES) analysis, recycling experiments, and a hot filtration test were conducted throughout the reaction to correlate the distribution of Pd between the solid and liquid

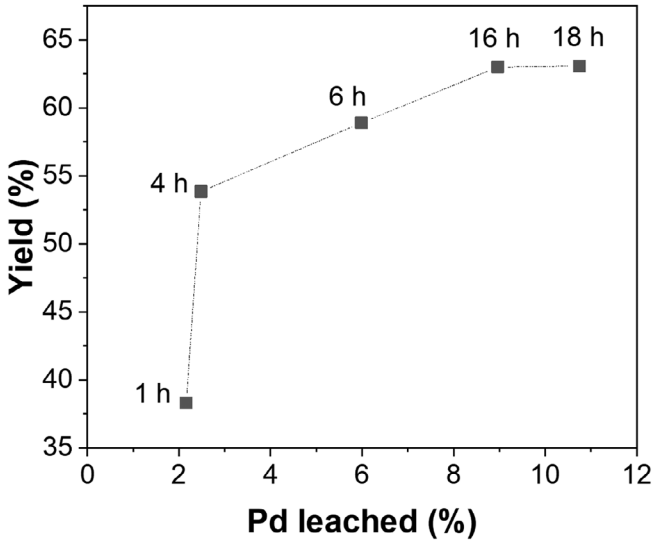

FIGURE 6 | Reaction product yields as a function of the amount of Pd leached into the solution over time.

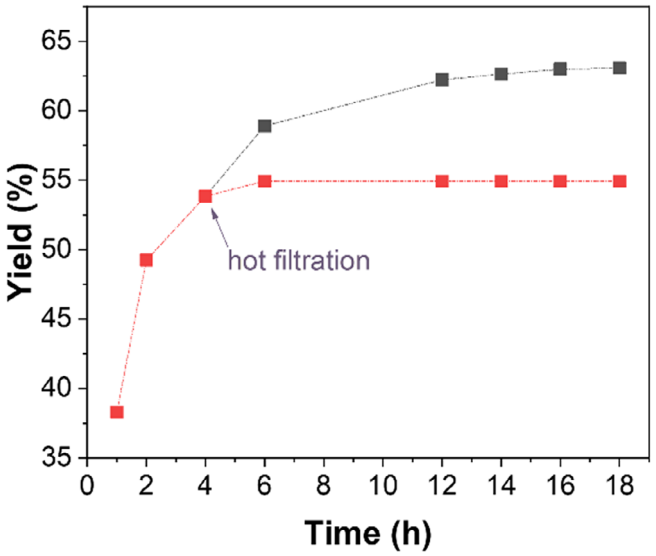

FIGURE 7 | Hot filtration test after 4 h reaction of the arylation of p-bromostyrene and diphenyliodonium triflate using PCP-Pd/SiO_2 as catalyst.

phases with the observed catalytic activity. As shown in Figure 6, a clear relationship was observed between product yield and the extent of Pd leaching up to 16 h: higher levels of Pd leached into solution corresponded to increased formation of *p*-bromostilbene. Beyond this point, the product yield remained unchanged despite continued Pd leaching. After 16 h of reaction, the residual Pd content in the solid phase was 0.89 wt.%, consistent with the amount detected in solution. Since the concentration of dissolved Pd did not decrease thereafter, it could be inferred that redeposition of Pd onto the solid support, commonly observed in cross-coupling systems [59], did not take place under these conditions. In this context, Tillou and Vannuci [60] recently reported a similar case in which the catalytic activity of a Pd-NNN pincer in benzyl alcohol hydrodeoxygenation was not inherent to the complex itself. Instead, the complex first evolved into an unsupported particulate catalyst, which subsequently acted as a reservoir for leached Pd species.

A hot filtration test, depicted in Figure 7, was performed after 4 h of reaction. Initially, a slight increase of about 2% in yield was observed, after which the yield remained constant throughout the reaction, suggesting that the solid phase is required to generate the active forms. When recycled, however, the solid material lost all catalytic activity after the first run, indicating that the Pd retained in the solid at the end of the reaction was no longer active. Taken together, these observations confirm the substantial structural changes of the initial Pd species. Although catalysis appears to be mainly driven by the fraction of Pd leached into solution, the solid component is necessary to progressively generate these soluble species. The leached Pd likely undergoes aggregation in solution, as inferred from the leaching experiments and from the fact that, after hot filtration, the solution-phase species could not promote further reaction, yet remained in the liquid phase according to the final Pd analysis of the solid.

Additionally, to better understand the role of surface hydroxyl groups in the catalyst structure and activity, we partially substituted the free -OH groups on SiO_2 using hexamethyldisilazane (HMDS) prior to Pd impregnation. The Pd loading was kept constant at approximately 0.98 wt.% Pd, as confirmed by ICP-OES. Two surface coverages were tested: one with HMDS added to achieve a final 1:1 OH-to-Pd molar ratio (PCP-Pd/SiO_2_HMDS_1:1), and another with excess HMDS to mask nearly all available surface hydroxyls (PCP-Pd/SiO_2_HMDS_exc). Under the optimized reaction conditions, the PCP-Pd/SiO_2_HMDS_1:1 catalyst showed a product yield of 38%, compared to 62% for the unmodified PCP-Pd/SiO_2 catalyst, representing a 40% drop in the catalytic activity. With the PCP-Pd/SiO_2_HMDS_exc catalyst, the yield dropped significantly to just 8%, similar to that of the homogeneous complex or its physical mixtures with the support. Inspection of the ^{29}Si NMR spectra of the catalysts (Figure S9 and Table S3) revealed that, even with excess HMDS, similar amounts of the reagent were grafted onto the silica surface. In the solid-state ^{31}P NMR spectra (Figure 8), in addition to the two signals observed in both Pd-POCOP-Cl and PCP-Pd/SiO_2 (as shown in Figure 1), the HMDS-modified catalysts, PCP-Pd/SiO_2_HMDS_1:1 and PCP-Pd/SiO_2_HMDS_exc, displayed an additional, broader resonance at approximately 144 ppm. This new signal suggests the presence of a distinct coordination environment between the complex and the support. Its higher intensity in the PCP-Pd/SiO_2_HMDS_exc sample implies that this species was more prevalent when more HMDS was present in the medium, even if not grafted onto the support. The 144-ppm signal appeared at a chemical shift similar to that of the homogeneous Pd-POCOP-Cl complex in solution, suggesting the presence of metal species with limited or no interaction with the support. This may result from steric hindrance imposed by grafted HMDS groups or residual silazane species loosely associated with the surface. Although quantification of the individual species was not feasible due to a low signal-to-noise ratio, the constant Pd content across all samples allowed us to infer that this less-interacting species competed with the formation of hydrogen-bonded or grafted Pd complexes. The presence of the 144-ppm signal correlated with the observed drop in catalytic performance indicates that the

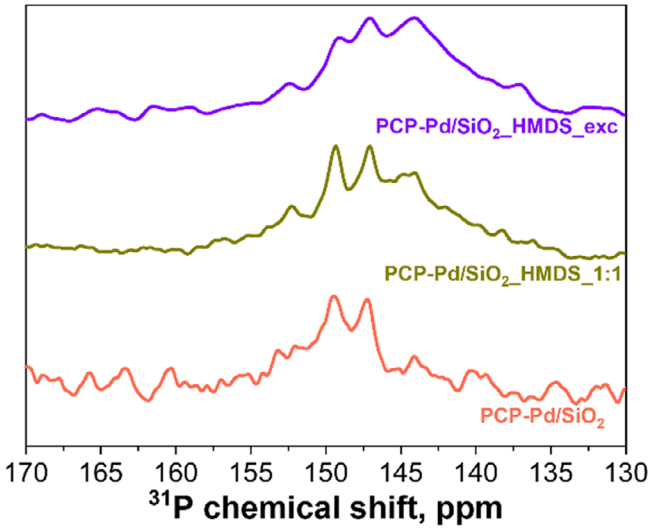

FIGURE 8 | Solid-state ^{31}P CP-MAS NMR spectra at 202.4 MHz and 10 kHz spinning rate for PCP-Pd/SiO_2, and surface-modified PCP-Pd/SiO_2_HMDS_1:1 and PCP-Pd/SiO_2_HMDS_exc.

hydrogen-bonded (O1 in Scheme 2) or grafted complexes (O2 in Scheme 2) were responsible for catalytic activity. These results strongly indicate that surface hydroxyl groups played a crucial role in affecting the nature of the surface species formed and, therefore, the catalytic outcome.

Building on the mechanism discussed in the literature for the homogeneous case [24] and supported by our experimental observations, we propose the catalytic cycle depicted in Scheme 3. Choosing as a starting point the most abundant hydrogen-bonded immobilized Pd-POCOP-Cl pincer complex (Scheme 3, O1), the cycle begins with it engaging in a Pd(II)/Pd(IV) cycle. Oxidative addition of diphenyliodonium triflate generates the Pd(IV) complex A, followed by styrene coordination and migratory insertion, referred to as carbopalladation, yielding the cationic Pd(IV) complex B. Subsequently, β-hydride elimination converts B into the Pd(IV)-hydride complex C. The deprotonation of C by the Na_2CO_3 base can restore the O1 species, closing the cycle. This pathway, predominant for the homogenous Pd-POCOP-Cl complex [24], appears, however, to be less efficient under the given conditions, as indicated by the low yields observed with the Pd-POCOP-Cl catalyst and its physical mixture with the support.

Consistent with the observations of Melero et al. [56], the Pd(IV)-hydride complex C can decompose, releasing Pd(0) species into solution and altering the surface composition. However, in our system, small amounts of Pd were gradually leached during the reaction, possibly in the form of dimeric (Scheme 3D) or polymeric (Scheme 3E) PCP-bridging Pd(0) complexes. In the solid phase, a mixture of adsorbed ligand decomposition product $Ph_2P(O)H$ and Pd(II)-phosphinate species are progressively formed. These species are catalytically inactive under the reaction conditions, as proven by the recycling tests. In solution, the leached Pd(0) complexes can further aggregate into small clusters that remain catalytically active via a Pd(0)/Pd(II) redox cycle. These molecular or small Pd clusters are likely the most active species under the reaction conditions. Over time, their evolution and agglomeration resulted in the formation of Pd black, a visible outcome during the reaction, and confirmed by the hot filtration test. This generation of highly active molecular and nanosized Pd species, arising from modifications of the initial solid catalyst, highlights the intricate interplay between homogeneous and heterogeneous pathways in the transformation.

3 | Conclusion

In this work, the heterogenization of a phosphinite-based PCP pincer Pd complex on silica was shown to preserve the pincer ligand coordination environment and the structural integrity of Pd-POCOP moiety. The resulting PCP-Pd/SiO_2 catalyst consisted predominantly of non-covalently immobilized species, with a small fraction covalently grafted onto the surface, and no evidence of metallic Pd. Under optimized conditions, catalytic and mechanistic studies revealed that the heterogeneous system outperformed its homogeneous analogue. This enhanced activity correlated with the gradual formation of small amounts of soluble Pd(0) species, in which the phosphine arms remained coordinated, while the solid phase evolved into catalytically inactive Pd(II)-phosphinate species and ligand degradation products upon recycling. Additionally, surface hydroxyl groups on the silica support were identified as key actors in mediating the formation of the active species. Lastly, a catalytic cycle was proposed, interconnecting Pd(II)/Pd(IV) and Pd(0)/Pd(II) pathways. These findings emphasize the intricate interplay between the surface complex and the support, highlighting the potential of surface hydroxyl groups in the design of efficient heterogeneous catalysts for redox transformations under mild conditions.

Acknowledgments

This work was funded in part by the São Paulo Research Foundation—FAPESP (DSL, 2022/11173-2; DZ, 2020/15230-5; GBS, 2020/12986-1; LSS, 2020/08575-6; JCP, 2021/06661-5; MOJ, 2022/02974-1; RPMF, 2023/07712-8), the Brazilian National Council for Scientific and Technological Development—CNPq (JCP, 308540/2021-2; DZ, 311226/2022-1; MOJ, 312802/2023-4), and the Coordination for the Improvement of Higher Education Personnel—CAPES (finance code 001). The authors thank the Brazilian Nanotechnology National Laboratory (LNNano), open national facilities operated by the Brazilian Center for Research in Energy and Materials (CNPEM) of the Brazilian Ministry for Science, Technology, Innovations, and Communications (MCTIC), for the access to XPS facilities (proposal 20240662), the Institute of Physics of the University of Sao Paulo (IFSC/USP), for the ^{31}P solid state NMR spectroscopy measurements, Dr. A.M. Beale from the UK Catalysis Hub at the Research Complex at Harwell, Didcot for the access to the DRIFTS analysis. The authors also thank the Multiuser Equipment Centre of IQ-UNICAMP (CEMUIQ) for access to the NMR equipment EMU-FAPESP (2022/11152-5).

The Article Processing Charge for the publication of this research was funded by the Coordenação de Aperfeiçoamento de Pessoal de Nível Superior - Brasil (CAPES) (ROR identifier: 00x0ma614).

Conflicts of Interest

The authors declare no conflict of interest.

Data Availability Statement

The data that support the findings of this study are available from the corresponding author upon reasonable request.

References

1. N. Selander and K. J. Szabó, "Catalysis by Palladium Pincer Complexes," *Chemical Reviews* 111 (2011): 2048–2076.

2. H. Valdés, E. Rufino-Felipe, and D. Morales-Morales, "Pincer Complexes, Leading Characters in C–H Bond Activation Processes. Synthesis and Catalytic Applications," *Journal of Organometallic Chemistry* 898 (2019): 120864, https://doi.org/10.1016/j.jorganchem.2019.07.015.

3. L. González-Sebastián and D. Morales-Morales, "Cross-Coupling Reactions Catalysed by Palladium Pincer Complexes. A Review of Recent Advances," *Journal of Organometallic Chemistry* 893 (2019): 39–51.

4. J. K. Liu, J. F. Gong, and M. P. Song, "Chiral Palladium Pincer Complexes for Asymmetric Catalytic Reactions," *Royal Society of Chemistry Preprint* 17 (2019): 6069–6098, https://doi.org/10.1039/c9ob00401g.

5. M. Ohff, A. Ohff, M. E. van der Boom, and D. Milstein, "Highly Active Pd(II) PCP-Type Catalysts for the Heck Reaction," *Journal of the American Chemical Society* 119 (1997): 11687–11688.

6. E. Marín-Carrillo, H. Valdés, S. Hernández-Ortega, and D. Morales-Morales, "Novel Hybrid Phosphinite-Theophylline Ligands and Their Pd(II) Complexes. Synthesis, Characterization and Catalytic Evaluation in Suzuki-Miyaura Couplings," *Inorganica Chimica Acta* 548 (2023): 121365, https://doi.org/10.1016/j.ica.2022.121365.

7. P. Jerome, P. N. Sathishkumar, N. S. P. Bhuvanesh, and R. Karvembu, "Towards Phosphine-Free Pd(II) Pincer Complexes for Catalyzing Suzuki-Miyaura Cross-Coupling Reaction in Aqueous Medium," *Journal of Organometallic Chemistry* 845 (2017): 115–124.

8. C. G. Martínez-De-León, A. Rodríguez-Álvarez, D. Morales-Morales, and J. M. Grévy, "Evaluation of Hemilabile Pd(II) NNS and NNSe Non-Symmetric Pincers in Suzuki–Miyaura Cross-Coupling: Unexpected Selective Nitrile Hydration of 4-bromonitrobenzene in Mild Conditions" *Journal of Organometallic Chemistry* 1011 (2024): 123103, https://doi.org/10.1016/j.jorganchem.2024.123103.

9. M. Bagherzadeh, N. alsadat Mousavi, M. Zare, S. Jamali, A. Ellern, and L. K. Woo, "ONO Pincer Type Binuclear Pd(II) Complex: Synthesis, Crystal Structure and Catalytic Utilization of the Resulting Organopalladium Complex in Catalytic Copper-Free Sonogashira Coupling Reaction," *Inorganica Chimica Acta* 451 (2016): 227–232.

10. S. Gu and W. Chen, "Pincer Complexes of Palladium- and Nickel-Containing 3-butyl-1-(1,10- phenanthrolin-2-yl)imidazolylidene as Efficient Aqueous Sonogashira and Kumada Coupling Reactions," *Organometallics* 28 (2009): 909–914.

11. D. Olsson, P. Nilsson, M. El Masnaouy, and O. F. Wendt, "A Catalytic and Mechanistic Investigation of a PCP Pincer Palladium Complex in the Stille Reaction," *Dalton Transactions* 11 (2005): 1924–1929.

12. H. Wang, J. Liu, Y. Deng, et al., "Pincer Thioamide and Pincer Thioimide Palladium Complexes Catalyze Highly Efficient Negishi Coupling of Primary and Secondary Alkyl Zinc Reagents at Room Temperature," *Chemistry—A European Journal* 15 (2009): 1499–1507.

13. X. Marset, S. De Gea, G. Guillena, and D. J. Ramón, "NCN–Pincer–Pd Complex as Catalyst for the Hiyama Reaction in Biomass-Derived Solvents," *ACS Sustainable Chemistry & Engineering* 6 (2018): 5743–5748.

14. A. Reyes-Deloso, J. G. Penieres-Carrillo, A. Toscano, et al., "Arylhydrazone-Thioeter Palladium Pincer Complexes Catalyzed Carbonylative Suzuki–Miyaura Cross-Coupling Using Fe(CO)5 as CO Surrogate" *Applied Organometallic Chemistry* 39 (2024): e7893, https://doi.org/10.1002/aoc.7893.

15. T. Wang, X. Q. Hao, J. J. Huang, K. Wang, J. F. Gong, and M. P. Song, "Chiral CNN Pincer Palladium(II) Complexes with 2-Aryl-6-(oxazolinyl)pyridine Ligands: Synthesis, Characterization, and Application to Enantioselective Allylation of Isatins and Suzuki–Miyaura Coupling Reaction," *Organometallics* 33 (2014): 194–205.

16. M. R. Eberhard, "Insights into the Heck Reaction with PCP Pincer Palladium(II) Complexes," *Organic Letters* 6 (2004): 2125–2128.

17. B. M. J. M. Suijkerbuijk, S. D. H. Martínez, G. Van Koten, and R. J. M. Klein Gebbink, "Hetero-multimetallic Tetrakis(SCS-pincer palladium)–(Metallo)Porphyrin Hybrids. Tunable Precatalysts in a Heck Reaction," *Organometallics* 27 (2008): 534–542.

18. A. Maji, A. Singh, A. Mohanty, P. K. Maji, and K. Ghosh, "Ferrocenyl Palladacycles Derived from Unsymmetrical Pincer-type Ligands: Evidence of Pd(0) Nanoparticle Generation During the Suzuki–Miyaura Reaction and Applications in the Direct Arylation of Thiazoles and Isoxazoles," *Dalton Transactions* 48 (2019): 17083–17096.

19. K. Gholivand, R. Salami, S. F. Rastegar, and S. M. Roe, "Dithiophosphorus-Palladium Complexes as a Catalyst in the Heck Reaction via Pd(II)/Pd(IV) Catalytic Cycle: a Combined Experimental and Computational Study," *ChemistrySelect* 3 (2018): 7822–7829.

20. B. L. Shaw, S. D. Perera, and E. A. Staley, "Highly Active, Stable, Catalysts for the Heck Reaction; Further Suggestions on the Mechanism," *Chemical Communications* 2 (1998): 1361–1362.

21. H. M. Lee, J. Y. Zeng, C. H. Hu, and M. T. Lee, "A New Tridentate Pincer Phosphine/ N -Heterocyclic Carbene Ligand: Palladium Complexes, Their Structures, and Catalytic Activities," *Inorganic Chemistry* 43 (2004): 6822–6829.

22. V. Saini, V. K. Madduluri, Pragya, K. Rangan, and B. Khungar, "Abnormal NHC Palladium(II) Complex Containing CNN Pincer Skeleton and Its Application to Suzuki-Miyaura Coupling of Aryl Chlorides in Water," *Asian Journal of Organic Chemistry* 12 (2023): e202300072, https://doi.org/10.1002/ajoc.202300072.

23. K. S. Yoo, J. O'Neill, S. Sakaguchi, R. Giles, J. H. Lee, and K. W. Jung, "Asymmetric Intermolecular Boron Heck-type Reactions via Oxidative Palladium(II) Catalysis with Chiral Tridentate NHC-Amidate-Alkoxide Ligands," *Journal of Organic Chemistry* 75 (2010): 95–101.

24. J. Aydin, J. M. Larsson, N. Selander, and K. J. Szabó, "Pincer Complex-Catalyzed Redox Coupling of Alkenes with Iodonium Salts via Presumed Palladium(IV) Intermediates," *Organic Letters* 11 (2009): 2852–2854.

25. G. Sabharwal, K. C. Dwivedi, C. Das, et al., "Detailed Mechanistic Studies on PNN-palladium Pincer Complex Catalyzed Suzuki-Miyaura Cross-Coupling Reaction Proceeding Through a PdII/PdIII/PdIV Catalytic Cycle," *Journal of Catalysis* 440 (2024): 115825, https://doi.org/10.1016/j.jcat.2024.115825.

26. J. Aydin and K. J. Szabó, "Palladium−Pincer Complex Catalyzed C−C Coupling of Allyl Nitriles With Tosyl Imines via Regioselective Allylic C−H Bond Functionalization," *Organic Letters* 10 (2008): 2881–2884.

27. K. J. Szabó, "Mechanism of the Oxidative Addition of Hypervalent Iodonium Salts to Palladium(II) Pincer-Complexes," *Journal of Molecular Catalysis A: Chemical* 324 (2010): 56–63.

28. A. J. Canty and A. Ariafard, "Computational Study Illustrating NCN-Palladium(IV) Involvement in Generating Pd0 Species to Facilitate Pd0/PdII Heck-Type Catalysis with Diphenyliodine(III) Species," *Organometallics* 42 (2023): 3227–3235.

29. N. Zohreh, S. H. Hosseini, M. Tavakolizadeh, C. Busuioc, and R. Negrea, "Palladium Pincer Complex Incorporation Onto the Fe3O4-entrapped Cross-Linked Multilayered Polymer as a High Loaded Nanocatalyst for Oxidation," *Journal of Molecular Liquids* 266 (2018): 393–404.

30. M. A. Goni, E. Rosenberg, S. Meregude, and G. Abbott, "A Methods Study of Immobilization of PONOP Pincer Transition Metal Complexes on Silica Polyamine Composites (SPC)," *Journal of Organometallic Chemistry* 807 (2016): 1–10.

31. G. Mohammadnezhad, M. Esfandiari, and F. Steiniger, "End-grafted Cu-NNN Pincer Complexes on PAMAM Dendrimers-SiO2: Synthesis and Characterization," *New Journal of Chemistry* 44 (2020): 15054–15065.

32. S. Liu, J. M. Tan, A. Gulec, et al., "Stabilizing Single-Atom and Small-Domain Platinum via Combining Organometallic Chemisorption and Atomic Layer Deposition," *Organometallics* 36 (2017): 818–828.

33. P. Zhang, S. Wu, J. Wang, et al., "Palygorskite-Mn(II): an Efficient and Recyclable Heterogeneous Catalyst for the Synthesis of Quinolines,"

Applied Clay Science 259 (2024): 108005, https://doi.org/10.1016/j.clay.2024.107518.

34. J. De Tovar, A. C. Ghosh, T. Di Santo, et al., "Electrochemical CO2 Reduction with a Heterogenized Iridium−Pincer Catalyst in Water," *ChemCatChem* 15 (2023): e202300049, https://doi.org/10.1002/cctc.202300049.

35. M. Esfandiari, G. Havaei, S. Zahiri, and G. Mohammadnezhad, "Pincer Complex Immobilization Onto Different Supports: Strategies and Applications," *Coordination Chemistry Reviews* 472 (2022): 214778, https://doi.org/10.1016/j.ccr.2022.214778.

36. K. Yu, W. Sommer, M. Weck, and C. W. Jones, "Silica and Polymer-tethered Pd?SCS-pincer Complexes: Evidence for Precatalyst Decomposition to Form Soluble Catalytic Species in Mizoroki?Heck Chemistry," *Journal of Catalysis* 226 (2004): 101–110.

37. K. Yu, W. Sommer, J. M. Richardson, M. Weck, and C. W. Jones, "Evidence That SCS Pincer Pd(II) Complexes Are Only Precatalysts in Heck Catalysis and the Implications for Catalyst Recovery and Reuse," *Advanced Synthesis & Catalysis* 347 (2005): 161–171.

38. W. J. Sommer, K. Yu, J. S. Sears, et al., "Investigations Into the Stability of Tethered Palladium(II) Pincer Complexes During Heck Catalysis," *Organometallics* 24 (2005): 4351–4361.

39. F. Rajabi, A. S. Burange, L. G. Voskressensky, and R. Luque, "Supported Phosphine Free Bis-NHC Palladium Pincer Complex: an Efficient Reusable Nanocatalyst for Suzuki-Miyaura Coupling Reaction," *Molecular Catalysis* 515 (2021): 111928, https://doi.org/10.1016/j.mcat.2021.111928.

40. H. Khandaka and R. K. Joshi, "Fe3O4@SiO2Supported Pd (II)-selenoether N-heterocyclic Carbene: a Highly Active and Reusable Heterogeneous Catalyst for C-O Cross-Coupling of Alcohols and Chloroarenes," *Tetrahedron Letters* 111 (2022): 154163, https://doi.org/10.1016/j.tetlet.2022.154163.

41. C. Gnad, A. Abram, A. Urstöger, F. Weigl, M. Schuster, and K. Köhler, "Leaching Mechanism of Different Palladium Surface Species in Heck Reactions of Aryl Bromides and Chlorides," *ACS Catalysis* 10 (2020): 6030–6041.

42. B. R. Vaddula, A. Saha, J. Leazer, and R. S. Varma, "A Simple and Facile Heck-Type Arylation of Alkenes with Diaryliodonium Salts Using Magnetically Recoverable Pd-catalyst," *Green Chemistry* 14 (2012): 2133–2136.

43. J. M. Pérez, R. Cano, G. P. McGlacken, and D. J. Ramón, "Palladium(II) Oxide Impregnated on Magnetite as a Catalyst for the Synthesis of 4-arylcoumarins: via a Heck-arylation/Cyclization Process," *RSC Advances* 6 (2016): 36932–36941.

44. I. J. S. Fairlamb, A. R. Kapdi, A. F. Lee, et al., "Mono- And Binuclear Cyclometallated Palladium(II) Complexes Containing Bridging (N,O-) and Terminal (N-) Imidate Ligands: Air Stable, Thermally Robust and Recyclable Catalysts for Cross-Coupling Processes," *Dalton Transactions* 23 (2004): 3970–3981.

45. B. Sheludko, M. T. Cunningham, A. S. Goldman, and F. E. Celik, "Continuous-Flow Alkane Dehydrogenation by Supported Pincer-Ligated Iridium Catalysts at Elevated Temperatures," *ACS Catalysis* 8 (2018): 7828–7841.

46. B. C. Vicente, Z. Huang, M. Brookhart, A. S. Goldman, and S. L. Scott, "Reactions of Phosphinites With Oxide Surfaces: a New Method for Anchoring Organic and Organometallic Complexes," *Dalton Transactions* 40 (2011): 4268–4274.

47. J. Willenbacher, O. Altintas, V. Trouillet, et al., "Pd-Complex Driven Formation of Single-Chain Nanoparticles," *Polymer Chemistry* 6 (2015): 4358–4365.

48. J. F. Moulder, W. F. Stickle, P. E. Sobol, and K. D. Bomben, *Handbook of X-Ray Photoelectron Spectroscopy* (Perkin-Elmer Corporation, 1992).

49. M. Brun, A. Berthet, and J. C. Bertolini, "XPS, AES and Auger Parameter of Pd and PdO," *Journal of Electron Spectroscopy and Related Phenomena* 104 (1999): 55–60.

50. A. B. Salah and D. Zargarian, "The Impact of P-substituents on the Structures, Spectroscopic Properties, and Reactivities of POCOP-Type Pincer Complexes of Nickel(ii)," *Dalton Transactions* 40 (2011): 8977.

51. A. V. Gaikwad and G. Rothenberg, "In-Situ UV-Visible Study of Pd Nanocluster Formation in Solution," *Physical Chemistry Chemical Physics* 8 (2006): 3669–3675.

52. M. Tromp, J. R. A. Sietsma, J. A. Van Bokhoven, et al., "Deactivation Processes of Homogeneous Pd Catalysts Using in Situ Time Resolved Spectroscopic techniques" *Chemical Communications* 1 (2003): 128–129.

53. J. A. Creighton and D. G. Eadon, "Ultraviolet–Visible Absorption Spectra of the Colloidal Metallic Elements," *Journal of the Chemical Society, Faraday Transactions* 87 (1991): 3881–3891.

54. O. Kühl, *Phosphorus-31 NMR Spectroscopy* (Springer, 2008).

55. C. Godinot, M. Gaysinski, O. P. Thomas, C. Ferrier-Pagès, and R. Grover, "On the Use of 31P NMR for the Quantification of Hydrosoluble Phosphorus-Containing Compounds in Coral Host Tissues and Cultured Zooxanthellae," *Scientific Reports* 6 (2016): 21760, https://doi.org/10.1038/srep21760.

56. C. Melero, L. M. Martínez-Prieto, P. Palma, D. Del Rio, E. Álvarez, and J. Cámpora, "Selective Reduction of a Pd Pincer PCP Complex to Well-Defined Pd(0) Species," *Chemical Communications* 46 (2010): 8851–8853.

57. R. B. Bedford, S. L. Hazelwood, M. E. Limmert, et al., "The Role of Ligand Transformations on the Performance of Phosphite- and Phosphinite-Based Palladium Catalysts in the Suzuki Reaction," *Organometallics* 22 (2003): 1364–1371.

58. Y. H. Cheng, C. M. Weng, and F. E. Hong, "Preparation of Monodentate Phosphinite Ligands: Their Applications in Palladium Catalyzed Suzuki Reactions," *Tetrahedron* 63 (2007): 12277–12285.

59. R. Redón, N. G. García-Peña, and C. C. Ocampo-Bravo, "Leaching of Atoms, Clusters, and Nanoparticles," *Recent Patents on Nanotechnology* 15 (2020): 125–141.

60. J. G. Tillou and A. K. Vannucci, "Determining the Active Catalytic Palladium Species Under Hydrodeoxygenation Conditions," *Journal of Organometallic Chemistry* 944 (2021): 121848, https://doi.org/10.1016/j.jorganchem.2021.121848.

61. M. Bielawski, M. Zhu, and B. Olofsson, "Efficient and General One-Pot Synthesis of Diaryliodonium Triflates: Optimization, Scope and Limitations," *Advanced Synthesis & Catalysis* 349 (2007): 2610–2618.

62. J. F. Gong, Y. H. Zhang, M. P. Song, and C. Xu, "New PCN and PCP Pincer Palladium(II) Complexes: Convenient Synthesis via Facile One-Pot Phosphorylation/Palladation Reaction and Structural Characterization," *Organometallics* 26 (2007): 6487–6492.

63. W. Kai, H. Qian, D. Liu, and Z. Ye, "NCN-Pincer Palladium Complexes Immobilized on MCM-41 Molecular Sieve: Application in A-arylation Reactions," *Molecular Catalysis* 462 (2019): 85–91.

64. L. Ding, Z. Chu, L. Chen, et al., "Pd-Salen and Pd-Salan Complexes: Characterization and Application in Styrene Polymerization," *Inorganic Chemistry Communications* 14 (2011): 573–577.

65. H. Sun, Q. Shen, and M. Yang, "New Neutral Ni(II)- and Pd(II)-based Initiators for Polymerization of Styrene," *European Polymer Journal* 38 (2002): 2045–2049.

66. G. Engelhardt and D. Michel, *High-Resolution Solid-State NMR of Silicates and Zeolites* (John Wiley & Sons, 1987).

Supporting Information

Additional supporting information can be found online in the Supporting Information section.

Supporting File 1: cctc70503-sup-0001-SuppMat.pdf.

The authors have cited additional references within the Supporting Information [61–66].